



AFRL-RY-WP-TP-2013-0025

**DELAY DIFFERENTIAL EQUATION-BASED MODELING
OF PASSIVELY MODE-LOCKED QUANTUM DOT
LASERS USING MEASURED GAIN AND LOSS SPECTRA
(POSTPRINT)**

Nicholas G. Usechak and Vassilios Kovanis

**Optoelectronic Technology Branch
Aerospace Components & Subsystems Division**

**Ravi Raghunathan, Mark T. Crowley, Sayan D. Mukherjee, and Luke F. Lester
University of New Mexico**

**Frédéric Grillot
Université Européenne de Bretagne**

**JANUARY 2013
Interim**

Approved for public release; distribution unlimited.

See additional restrictions described on inside pages

© 2011 SPIE

STINFO COPY

**AIR FORCE RESEARCH LABORATORY
SENSORS DIRECTORATE
WRIGHT-PATTERSON AIR FORCE BASE, OH 45433-7320
AIR FORCE MATERIEL COMMAND
UNITED STATES AIR FORCE**

REPORT DOCUMENTATION PAGE					Form Approved OMB No. 0704-0188	
<p>The public reporting burden for this collection of information is estimated to average 1 hour per response, including the time for reviewing instructions, searching existing data sources, gathering and maintaining the data needed, and completing and reviewing the collection of information. Send comments regarding this burden estimate or any other aspect of this collection of information, including suggestions for reducing this burden, to Department of Defense, Washington Headquarters Services, Directorate for Information Operations and Reports (0704-0188), 1215 Jefferson Davis Highway, Suite 1204, Arlington, VA 22202-4302. Respondents should be aware that notwithstanding any other provision of law, no person shall be subject to any penalty for failing to comply with a collection of information if it does not display a currently valid OMB control number. PLEASE DO NOT RETURN YOUR FORM TO THE ABOVE ADDRESS.</p>						
1. REPORT DATE (DD-MM-YY) January 2013		2. REPORT TYPE Technical Paper		3. DATES COVERED (From - To) 15 September2008 – 22 March 2012		
4. TITLE AND SUBTITLE DELAY DIFFERENTIAL EQUATION-BASED MODELING OF PASSIVELY MODE-LOCKED QUANTUM DOT LASERS USING MEASURED GAIN AND LOSS SPECTRA (POSTPRINT)				5a. CONTRACT NUMBER In-house		
				5b. GRANT NUMBER		
				5c. PROGRAM ELEMENT NUMBER 61102F		
6. AUTHOR(S) Nicholas G. Usechak and Vassilios Kovanis (AFRL/RYPDH) Ravi Raghunathan, Mark T. Crowley, Sayan D. Mukherjee, and Luke F. Lester (University of New Mexico) Frédéric Grillot (Université Européenne de Bretagne)				5d. PROJECT NUMBER 2305		
				5e. TASK NUMBER DP		
				5f. WORK UNIT NUMBER Y05T		
7. PERFORMING ORGANIZATION NAME(S) AND ADDRESS(ES) Optoelectronic Technology Branch Aerospace Components & Subsystems Division Air Force Research Laboratory, Sensors Directorate Wright-Patterson Air Force Base, OH 45433-7320 Air Force Materiel Command, United States Air Force				University of Mexico Université Européenne de Bretagne 8. PERFORMING ORGANIZATION REPORT NUMBER AFRL-RY-WP-TP-2013-0025		
9. SPONSORING/MONITORING AGENCY NAME(S) AND ADDRESS(ES) Air Force Research Laboratory Sensors Directorate Wright-Patterson Air Force Base, OH 45433-7320 Air Force Materiel Command United States Air Force		Air Force Office of Scientific Research (AFOSR) National Science Foundation (NSF) Defense Threat Reduction Agency (DTRA)		10. SPONSORING/MONITORING AGENCY ACRONYM(S) AFRL/RYPDH		
				11. SPONSORING/MONITORING AGENCY REPORT NUMBER(S) AFRL-RY-WP-TP-2013-0025		
12. DISTRIBUTION/AVAILABILITY STATEMENT Approved for public release; distribution unlimited.						
13. SUPPLEMENTARY NOTES Journal article published in Proc. SPIE Photonics West, Vol 8255, 2012. ©2012 SPIE. The U.S. Government is joint author of the work and has the right to use, modify, reproduce, release, perform, display or disclose the work. PAO Case Number 88ABW-2012-0436, Clearance Date 30 January 2012. Report contains color.						
14. ABSTRACT A highly tunable millimeter-wave subcarrier signal is generated by optically injecting a Fabry–Perot semiconductor laser. The optically injected light, which enables microwave subcarrier frequencies well beyond the injected laser’s free-running relaxation oscillation frequency, is then on–off keyed by direct-current (dc) modulation of the injected slave laser. Adjustment of the subcarrier frequency is easily accomplished by changing either the dc bias current and/or junction temperature of the injected slave or the injecting master laser. In this paper, we theoretically and experimentally investigate the purity of the modulated microwave subcarrier. The generated microwave signal was then transmitted over 50 km of single-mode fiber, demonstrating the applicability of a directly modulated slave laser optically injected into the period-one state for radio-over-fiber applications.						
15. SUBJECT TERMS Semiconductor lasers, quantum dots, delay differential equation, passive mode-locking, linewidth-enhancement factor.						
16. SECURITY CLASSIFICATION OF:			17. LIMITATION OF ABSTRACT: SAR	18. NUMBER OF PAGES 12	19a. NAME OF RESPONSIBLE PERSON (Monitor) Nicholas Usechak 19b. TELEPHONE NUMBER (Include Area Code) N/A	
a. REPORT Unclassified	b. ABSTRACT Unclassified	c. THIS PAGE Unclassified				

Delay Differential Equation-Based Modeling of Passively Mode-Locked Quantum Dot Lasers Using Measured Gain and Loss Spectra

Ravi Raghunathan^{1,*}, Mark T. Crowley¹, Frédéric Grillot^{2,3}, Sayan D. Mukherjee¹, Nicholas G. Usechak⁴, Vassilios Kovanis⁴, Luke F. Lester¹

¹Center for High Technology Materials, University of New Mexico, 1313 Goddard SE, Albuquerque, NM 87108

²Université Européenne de Bretagne, INSA, CNRS- Laboratoire FOTON, UMR 6082, 20 avenue des buttes de Coesmes, 35708 Rennes, Cedex 7, France

³Telecom Paristech, Ecole National Supérieure des Télécommunications, CNRS LTCI, 75634 Paris Cedex, France

⁴Air Force Research Laboratory, 2241 Avionics Circle, Wright – Patterson AFB, Dayton, OH 45433

ABSTRACT

In this paper, we investigate the dynamics of a nonlinear delay differential equation model for passive mode-locking in semiconductor lasers, when the delay model is seeded with parameters extracted from the gain and loss spectra of a quantum dot laser. The approach used relies on narrowing the parameter space of the model by constraining the values of most of the model parameters to values extracted from gain and loss measurements at threshold. The impact of the free parameters, namely, the linewidth enhancement factors that are not available from the gain and loss measurements, on the device output is then analyzed using the results of direct integration of the delay model. In addition to predicting experimentally observed trends such as pulse trimming with applied absorber bias, the simulation results offer insight into the range of values of the linewidth enhancement factors in the gain and absorber sections permissible for stable mode-locking near threshold. Further, the simulations show that this range of permissible values progressively decreases with increasing bias voltage on the absorber section. This is important for telecom and datacom applications where such devices are sought as pulsed sources, as well as in military RF photonic applications, where mode-locked diode lasers are used as low noise clocks for sampling.

Keywords: Semiconductor lasers, quantum dots, delay differential equation, passive mode-locking, linewidth enhancement factor.

1. INTRODUCTION

Quantum dot mode-locked lasers (QDMLs) are attractive optical sources for applications requiring pulse trains with low timing jitter and low energy per bit, such as optical interconnects in multi-processor architectures^{1, 2}. In order to optimize QDMLs for these precision applications, it is necessary to accurately predict device operation using realistic parameters characteristic of the underlying semiconductor gain material, under realistic operating conditions. To this end, certain properties distinctive to QD systems, such as low linewidth enhancement factors and reduced values of unsaturated gain and absorption^{3, 4}, if understood and exploited properly, could offer considerable performance benefits over bulk and quantum well (QW)-based systems. For instance, quantitative knowledge of the bias conditions under which a device will generate stable pulses with good quality is highly desirable for any application where stable pulses are desired under variable operating conditions. A typical example of such an application is the possible use of QDMLs as pulsed sources in operating environments such as data centers (where uncooled QDMLs are sought as sources of stable pulses) that require components to be able to tolerate high temperatures accompanied by rapid and considerable

*raghunat@unm.edu; Phone: (505) 272-7931; Fax: (505) 272-7801

Physics and Simulation of Optoelectronic Devices XX, edited by Bernd Witzigmann, Marek Osinski, Fritz Henneberger, Yasuhiko Arakawa, Proc. of SPIE Vol. 8255, 82551K
© 2012 SPIE · CCC code: 0277-786X/12/\$18 · doi: 10.1117/12.910007

Proc. of SPIE Vol. 8255 82551K-1

heat generation within the system. Consequently, devices need to be engineered to be able to sustain stable output pulses over a range of operating conditions^{5,6}.

In order to design and engineer devices that can meet the stringent restrictions of such precision applications, robust modeling techniques are highly desirable. And while a considerable amount of effort has gone into developing detailed analytical and numerical models to describe mode locking in semiconductor lasers (and even modified specifically for QDMLLs), the information available in the literature about device parameter values unique to QD-based structures and how they can be accessed and exploited so as to optimize device performance, is very limited. This has led to the associated theoretical and experimental work following two distinct paths, with the former focusing on developing analytical/numerical models of varying degrees of complexity to describe specific physical processes/phenomena constituting the mode-locking process, while the latter typically relies on a process of iterative design through extensive testing and characterization. On the theoretical side, as more physical effects and processes are incorporated into the analysis, the model grows in complexity and evolves to encompass a large parameter space. Although this added complexity should enable a better understanding of the underlying device physics and operation, the lack of easily measurable values, coupled with the number of required parameters often limits the practical utility of more rigorous models.

Previously, we used a Delay Differential Equation (DDE) model for passive mode locking in semiconductor lasers^{7,8,9} to analyze the asymmetry inherent in the output pulses generated by QDMLLs¹⁰. In this paper, the DDE model is used to study the impact of the linewidth enhancement factor in the gain and saturable absorber sections on the steady state device output. The use of a system of differential equations incorporating a delay term as opposed to a system of partial differential equations enables a reduced parameter space and computational simplicity¹¹. To this end, physical quantities measured from the gain and loss spectra of the QD substrate material are transformed into model parameters, which are then used as initial conditions to seed the model. Relative to the other models used to study passive mode locking in semiconductor lasers, the DDE model has a parameter space of just 9 parameters, most of which can be extracted from measurable physical quantities, leaving only a small number of free parameters^{12,13,14}. This enables seeding the model with realistic input parameters for each operating condition. The linewidth enhancement factors in the gain and absorber sections, which are not available from the gain and loss data, are then left as free parameters that can be varied to study changes in device output. Getting a sense of the linewidth enhancement factor of a device operating under a certain set of conditions is important, because it is indicative of the frequency chirp in the system, and QDMLLs with low chirp are highly desirable for telecommunications applications¹⁵. Also, numerical analysis has shown that in the case of a QDMLL operating under optical feedback, the role of the linewidth enhancement factor in the gain and absorber sections is a key determining factor for the mode-locking dynamics¹⁶.

However, experimental measurement techniques are known to yield widely varying results, depending on the technique used and the biasing conditions¹⁷. Consequently, experiments have reported values ranging from very small¹⁸ to very large¹⁹. For this reason, it is highly desirable to have a numerical model that can predict an estimated range of values that the linewidth enhancement factor can take, under a certain set of operating conditions.

In addition to giving insight into the range of permissible values that the linewidth enhancement factor can take, the simulations are shown to predict key experimental trends, such as pulse trimming for an applied bias voltage. The primary objective of this work is to show that the DDE model, used in its original form without any modifications and seeded with parameter values extracted from actual gain and loss measurements on the constituent QD material, provides a highly useful guide to predict and analyze device performance.

2. THEORETICAL BACKGROUND

The Delay Differential Equation (DDE) model due to Vladimirov and Turaev is derived from the standard coupled Partial Differential Equation (PDE) formalism, which describes the interaction of a slowly varying complex optical field with the carrier densities in the gain and absorber sections of a generic semiconductor laser^{8,9}:

$$\frac{dA(\tau)}{d\tau} = \gamma\sqrt{\kappa}e^{\left\{\frac{1}{2}(-i\alpha_g)G(\tau-T) - \frac{1}{2}(-i\alpha_a)D(\tau-T)\right\}}A(\tau-T) - \gamma A(\tau) \quad (1)$$

$$\frac{dG(\tau)}{d\tau} = g_0 - \Gamma G(\tau) - e^{-Q(\tau)}(e^{G(\tau)} - 1)A(\tau)^2 \quad (2)$$

$$\frac{dQ(\tau)}{d\tau} = q_0 - Q(\tau) - s(1 - e^{-Q(\tau)})A(\tau)^2 \quad (3)$$

In equations (1)–(3) above, γ incorporates the effect of spectral filtering, α_g and α_q are the linewidth enhancement factors in the gain and absorber media respectively, and κ accounts for linear cavity losses. The delay parameter incorporates history, which appears in the first equation of the model through the evaluation of optical field A , saturable gain G , and saturable loss Q at the times $\tau - T$, where T denotes the normalized round trip time. Parameter $\Gamma = (\tau_{abs}/\tau_{gain})$ is the ratio between the absorber and gain relaxation times, and s is the saturation parameter. Finally, g_0 and q_0 are the unsaturated gain and absorption, respectively.

A recent experiment⁶ has shown that the segmented contact method^{20, 21} can be used to obtain modal gain and total loss spectra as a function of absorber bias voltage and temperature for the QD material comprising the device. These curves were used to extract the modal gain (g_{mod}) and unsaturated absorption (a_0) as a function of current density at each absorber bias condition. In the following, a systematic method to transform physically measured parameters from the gain and loss spectra into seed conditions for the DDE model is discussed.

Now, from equation (2) in [6], the threshold condition for lasing can be expressed as follows,

$$(g_{mod}(J) - \alpha_i)L_g - (a_0 + \alpha_i)L_a = \alpha_m(L_a + L_g) \quad (4)$$

where, α_m and α_i represent, respectively, mirror losses and internal losses, and L_g and L_a represent, respectively, the gain and absorber section lengths, with:

$$\alpha_m = \left(\frac{1}{L}\right) \ln\left(\frac{1}{\sqrt{R_1 R_2}}\right) \quad (5)$$

where, $(L_g + L_a) = L$ and R_1, R_2 denote mirror reflectivities.

In the DDE model, G and Q describe the saturable gain and loss introduced by the gain and absorber sections, respectively, and $\kappa < 1$ describes the total roundtrip non-resonant linear intensity losses. Thus, the threshold condition for lasing is given by⁹:

$$\kappa e^{(G-Q)} = 1 \Rightarrow G = Q - \ln(\kappa) \quad (6)$$

Comparing (3) and (4), we find:

$$G_{threshold} = (g_{mod}(J) - \alpha_i)L_g \quad (7)$$

$$Q_{threshold} = (a_0 + \alpha_i)L_a \quad (8)$$

$$\kappa = \sqrt{R_1 R_2} \quad (9)$$

A key feature of the DDE model is its dimensionless formalism, whereby physically measured laser parameters must be scaled appropriately and made dimensionless, before being used as inputs to the model. Thus, in order to enable a direct conversion between measurable static laser quantities and the definitions appearing in [9], transformation relations to relate the saturable gain and absorption (G and Q , respectively) to the corresponding unsaturated parameters (g_0 and q_0 , respectively) have been derived to yield:

$$g_0 = \Gamma G \quad (10)$$

$$q_0 = (Q/s) \quad (11)$$

where,

$$s \equiv \frac{g_q \Gamma_q}{g_g \Gamma_g} = \frac{[\partial g_{\text{mod}}(J)/\partial J]_{g_{\text{mod}}(J)=0}}{[\partial g_{\text{mod}}(J)/\partial J]} \quad (12)$$

Further, using the dynamical stability analysis presented in Fig. 5 of [9], it is deduced that a suitable constraint to achieve stable, fundamental mode-locking in terms of g_0 and q_0 , yields an expression for the carrier relaxation ratio, Γ , which depends solely on measurable static device parameters defined above in equations (7), (8) and (12):

$$\Gamma = \left(\frac{Q}{2Gs} \right) = \frac{(a_0 + \alpha_i)L_a}{2(g_{\text{mod}}(J) - \alpha_i)L_g s} \quad (13)$$

Equations (7) – (13) provide a set of initial conditions that can be used to seed the simulation.

3. SIMULATION RESULTS

In this section, the simulation results for an 8-stack InAs dots-in-a-well (DWELL) passively mode locked laser, with a 1 mm absorber section and 7 mm gain section are presented. The details of device structure, experimental data and results can be found in [6]. The approach involves extracting parameters appearing on the right sides of equations (7), (8), (12) and (13) from quantities measured as a function of gain-section current density, wavelength, absorber reverse bias and temperature using the segmented contact method^{20, 21}.

This method of parameter extraction provides an extremely convenient technique to determine model parameters for input into the DDE model. Such a situation may be envisioned for a case where device performance needs to be simulated over a range of temperatures and operating conditions. In such cases, the benefits of being able to accurately simulate the output characteristics of a proposed device, with no more than a relatively simple set of gain and loss measurements on a test structure (and parameters extracted from these), and using the results to guide device engineering can be clearly seen to be invaluable. Conversely, the simulation results can offer invaluable insight into the range of values a given parameter can take, in order for device operation to be stable. For instance, if the values extracted for the unsaturated gain and absorption are raised by a factor of ten each (while all other parameter values are retained), the simulation yields unstable pulses. In this section, simulation results obtained by seeding the model with parameters extracted from physically measured quantities are presented and discussed.

A close examination of the system of DDEs given in equations (1)-(3) reveals the parameter space involved. Thus, in order to model a QDMLL realistically, it is imperative to constrain as many of the parameters as possible to values typical of a QD device. Since the onset of lasing occurs at threshold, the first step is to use values measured at threshold in equations (7) and (8) to calculate $G(0)$ and $Q(0)$, and then use the values of $G(0)$ and $Q(0)$ in equations (10) and (11) to calculate the corresponding unsaturated parameters, g_0 and q_0 at threshold. Further, parameters κ and s can be directly found from equations (9) and (12) respectively, while the carrier relaxation ratio (Γ) is extracted from equation (13). The delay parameter T is determined for each set of operating conditions by scaling the cavity round trip time to the corresponding absorber recovery time, which is chosen as the characteristic timescale. Of the remaining three model parameters, the spectral filtering coefficient (γ) was judiciously chosen and held constant, while the values of linewidth enhancement factor in the gain and absorber sections were varied in tandem. Thus, the main assumptions made to simplify the analysis were: 1.) the spectral filtering was assumed to be invariant with respect to the gain and linewidth enhancement factors, and 2.) the linewidth enhancement factors in the gain and absorber sections were kept equal.

The results shown in the following were obtained as follows. The parameter values measured/extracted as discussed above were used as initial conditions for the simulations. The system of equations defining the model (equations (1), (2) and (3)) was then integrated over several round trip times to allow transients to settle. The primary objective was

to constrain as many of the model parameters as possible to measured values, so as to get a sense of the range of values that the non-measured parameters (namely, the linewidth enhancement factors in the gain and absorber sections) can take under the operating conditions under study. Stable device operation is simulated as stable, fundamental mode locking (identical pulses, once every round trip), so that any variation in pulse amplitude, duration or structure, or multiple pulses in a round trip are representative of a breakdown of the device output. Table I lists a sample set of parameter values, extracted from gain and loss spectra at 20 C and no applied absorber bias at threshold (current density = 357 A/cm²). The delay parameter T has been scaled using a characteristic timescale of 62 ps, which was inferred from measurements performed on a QD saturable absorber with a similar epitaxial structure²², using an equivalent value of active region field strength.

Table I: Simulation Parameters at 20 C, 0 V Absorber Bias ($\alpha_g = \alpha_q = 2.5$)

$T = 3.226$	$G(0) = 3.33$	$Q(0) = 2.33$
$\alpha_g = 2.5$	$\alpha_q = 2.5$	$s = 2.676$
$\Gamma = 0.13$	$\gamma = 13.3$	$\kappa = 0.55$

The values of α_g and α_q shown are for one particular case. They have been chosen equal based on the analysis presented in [9], where it was numerically shown that the best pulse quality is achieved for the case of equal values of linewidth enhancement factor in the gain and absorber sections.

Fig. 1a shows the steady state output of the system of equations in (1)-(3), for the case $\alpha_g = \alpha_q = 2.5$.

In the absence of an applied bias on the absorber section, there is no sweep-out mechanism as a result of the associated electric field to expedite the carrier relaxation rate in the absorber section. Thus, the absorber takes a longer time to recover, resulting in sub-optimal pulse trimming. Thus, the simulation results predict broad pulses, with a width ~ 23 ps (Fig. 1b).

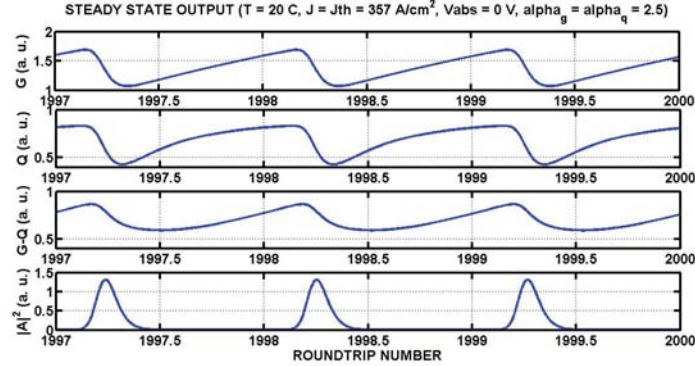


Fig. 1a: Steady state output for 0 V absorber bias, $\alpha_g = \alpha_q = 2.5$: $G(\tau)$, $Q(\tau)$, $(G(\tau)-Q(\tau))$ and $|A(\tau)|^2$.

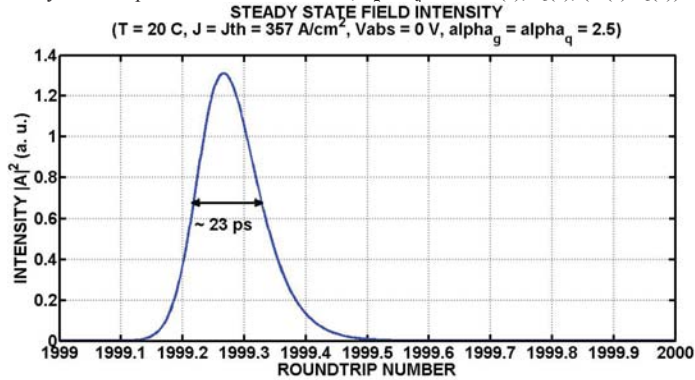


Fig. 1b: Steady state pulse intensity profile for 0 V absorber bias, $\alpha_g = \alpha_q = 2.5$.

Further, the mode-locked pulses are predicted to become unstable for $\alpha_g = \alpha_q = 2.9$ (Fig. 1c). This is evidenced by the unequal pulse intensities, along with the appearance of a pronounced side structure on the leading edge of each pulse.

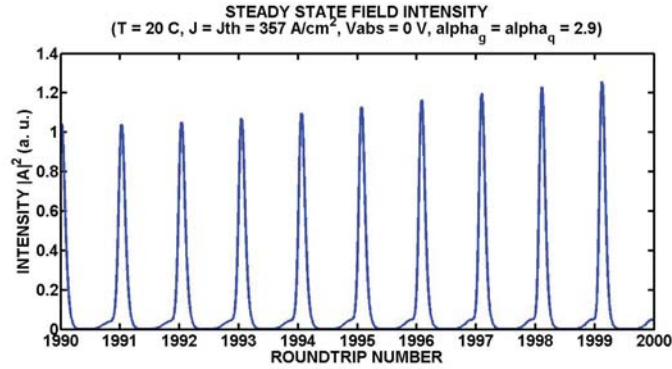


Fig. 1c: Steady state field intensity $|A(\tau)|^2$ for 0 V absorber bias, $\alpha_g = \alpha_q = 2.9$.

It may be noted that mild instabilities were obtained for the cases where the α -parameters were chosen to be greater than 2.5. The case $\alpha_g = \alpha_q = 2.9$ is shown here to elucidate the nature of typical instabilities.

Thus, the simulation results show that for the combination of parameters extracted at 20 C with no applied reverse bias, the values of linewidth enhancement factor in the gain and absorber sections must be less than or equal to 2.5, in order to ensure stable, fundamental mode-locking.

Next, the effect of an applied (moderate) bias voltage is considered, with $V_{\text{abs}} = -3\text{V}$. Again, in this case, all other parameters are constrained to extracted values, and the effect of the linewidth enhancement factor is analyzed by simulation. Table II lists a sample set of parameter values, extracted from gain and loss spectra at 20 C and an applied absorber bias of -3V at threshold (current density = 462 A/cm²). Again, using the measurements reported in [22], the delay parameter T was scaled to a characteristic timescale of 40 ps.

Table II: Simulation Parameters at 20 C, -3 V Absorber Bias ($\alpha_g = \alpha_q = 1.8$)

$T = 5.0$	$G(0) = 4.18$	$Q(0) = 3.20$
$\alpha_g = 1.8$	$\alpha_q = 1.8$	$s = 4.65$
$\Gamma = 0.08$	$\gamma = 13.3$	$\kappa = 0.55$

Fig. 2a shows the simulation output for the case $\alpha_g = \alpha_q = 1.8$. Compared to the previous case with no applied bias, the net gain profile in the third panel shows a sharper profile, suggesting a shorter interval of high net gain – this is seen as considerably better trimmed pulses in the fourth panel, with a pulse width ~ 10 ps (Fig. 2b).

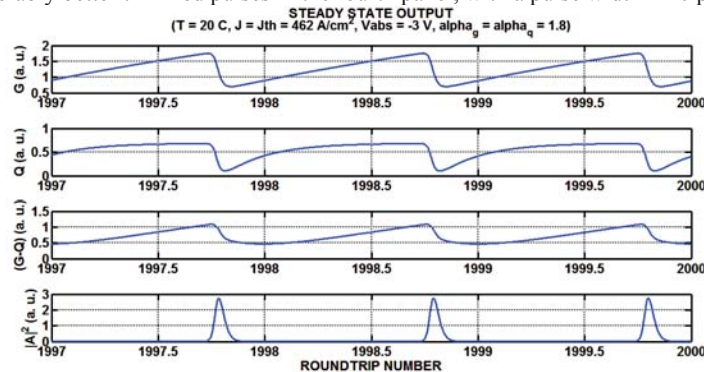


Fig. 2a: Steady state output for -3 V absorber bias, $\alpha_g = \alpha_q = 1.8$: $G(\tau)$, $Q(\tau)$, $(G(\tau)-Q(\tau))$ and $|A(\tau)|^2$.

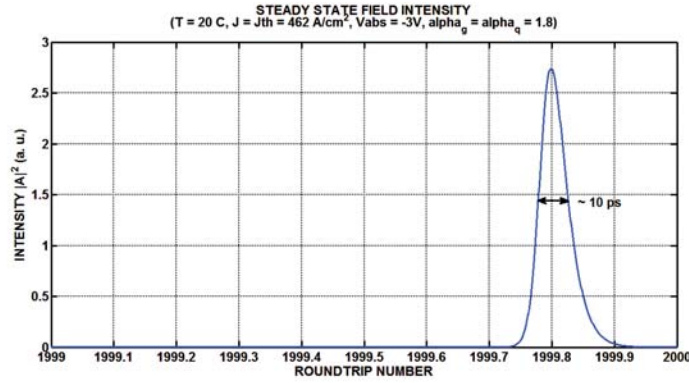


Fig. 2b: Steady state pulse intensity profile for -3 V absorber bias, $\alpha_g = \alpha_q = 1.8$.

In this case, the simulation results predict that instabilities begin to appear in the mode-locked pulses for $\alpha_g = \alpha_q = 1.9$ (Fig. 2c), as seen from the variable pulse intensities.

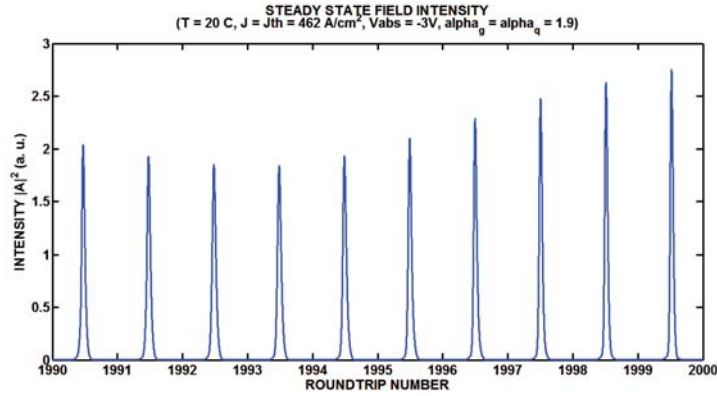


Fig. 2c: Steady state field intensity $|A(\tau)|^2$ for -3 V absorber bias, $\alpha_g = \alpha_q = 1.9$.

Finally, we consider the effect of a strong applied bias of -5 V on the absorber section. Table III lists a sample set of parameter values, extracted from gain and loss spectra at 20 C and an applied absorber bias of -5V at threshold (current density = 537 A/cm²). Again, using the measurements reported in [22], the delay parameter T was scaled to the characteristic timescale, chosen to correspond to an absorber recovery time of 30 ps.

Table III: Simulation Parameters at 20 C, - 5 V Absorber Bias ($\alpha_g = \alpha_q = 0.8$)

$T = 6.667$	$G(0) = 4.55$	$Q(0) = 3.62$
$\alpha_g = 0.8$	$\alpha_q = 0.8$	$s = 6.90$
$\Gamma = 0.0576$	$\gamma = 13.3$	$\kappa = 0.55$

Fig. 3a shows the simulation output for the case $\alpha_g = \alpha_q = 0.8$.

In this case, we find, comparing the first and second panels in Fig. 3a to the corresponding panels in Fig. 2a, that while the saturable gain profile in both cases follows a similar trend, the saturable loss saturates at a lower value for a higher bias. The lower losses lead to a slightly higher net gain window than the -3 V case, so that pulses are trimmed to ~ 8.75 ps (Fig. 3b).

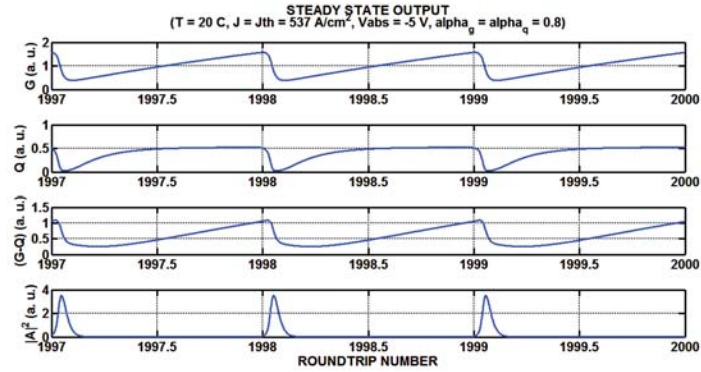


Fig. 3a: Steady state output for -5 V absorber bias, $\alpha_g = \alpha_q = 0.8$: $G(\tau)$, $Q(\tau)$, $(G(\tau)-Q(\tau))$ and $|A(\tau)|^2$.

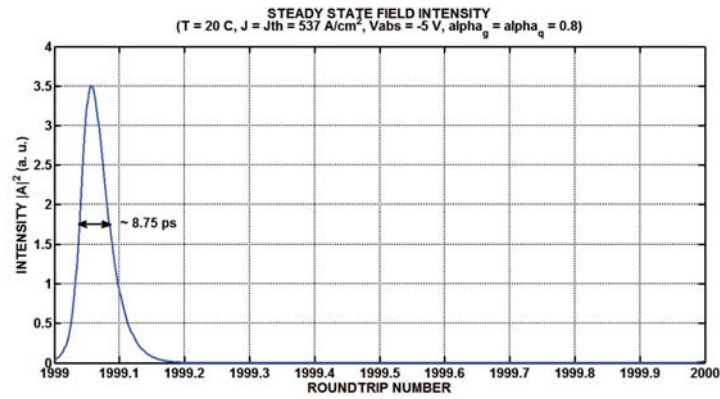


Fig. 3b: Steady state pulse intensity profile for -5 V absorber bias, $\alpha_g = \alpha_q = 0.8$.

Interestingly, the onset of instabilities in this case appears at $\alpha_g = \alpha_q = 0.9$ as an abrupt switch from fundamental to second-order mode-locking (Fig. 3c). This change of operating regime is characterized by the sudden appearance of two pulses every round trip. Physically, this represents a breakdown of stable, fundamental mode-locking.

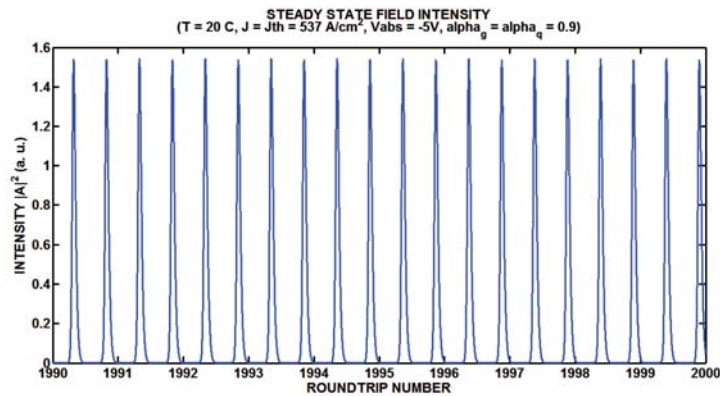


Fig. 3c: Steady state field intensity $|A(\tau)|^2$ for -5 V absorber bias, $\alpha_g = \alpha_q = 0.9$.

A comparison between Fig. 1a, 2a and 3a shows that the impact of increasing absorber bias voltage is a slight sharpening of the saturable gain and loss profiles, so that a slightly higher peak gain coincides with a slightly lower

loss in the latter case, resulting in larger net gain in a shorter time window. This is predicted to lead to narrower pulses.

Further, the application of a bias voltage not only trims the output pulses considerably, but also results in a decreased range of possible values of the linewidth enhancement factor in order to maintain stable mode-locking.

Thus, the range of possible values of α_g and α_q extends to 2.5 when no reverse bias is applied, but is restricted to 1.8 or less when a moderate bias of -3 V is applied, and 0.8 or less when a strong bias of -5 V is applied.

4. CONCLUSIONS

A Delay Differential Equation-based approach has been used to model a two-section, passively mode-locked quantum dot laser, where most of the model parameters have been extracted from gain and loss measurements performed on the quantum dot substrate. The objective was to get a sense of the linewidth enhancement factor in the gain and absorber sections distinctive to the particular QD device operating under a certain set of conditions, in order to ensure stable, fundamental mode-locking. To this end, the parameters that were not obtainable from the gain and loss measurements, namely, the linewidth enhancement factors in the gain and absorber sections, were varied and their impact on the device output was studied at a constant temperature of 20 °C, for the cases of no applied bias, moderate bias (-3V) and strong bias (-5V) on the absorber section. The key simplifying assumptions were to keep the spectral filtering coefficient invariant with respect to the gain and linewidth enhancement factors, and to consider equal values of linewidth enhancement factors in the gain and absorber sections. The simulation results not only predicted the experimentally-observed trend of pulse narrowing with applied bias, but also that stable mode locking is restricted to a narrow range of possible values of the linewidth enhancement factors, before either the pulses become unstable, or the device switches to higher-order mode locking. Further, the results showed that this range is significantly reduced with the application of a moderate bias (and reduced even further for a strong bias), which is important for telecom and datacom applications, as well as for military RF photonic applications such as low noise clocks.

ACKNOWLEDGEMENTS

This work was supported in part by the NSF under grant ECCS-0903448, by DTRA under grant DTRA01-03-D-0009-0026, by AFOSR under grant FA9550-1-10-0276 and by the SRC under contract SRC-2009-HJ-2000. N. G. Usechak and V. Kovanis were funded by the AFOSR.

REFERENCES

- [1]. Keeler, G. A., Nelson, B. A., Agrawal, D., Debaes, C., Helman, N. C., Bhatnagar, A. and Miller, D. A. B., "The benefits of ultrashort optical pulses in optically interconnected systems", IEEE J. Sel. Top. Quantum Electron. 9, 477-485 (2003).
- [2]. Miller, D. A. B., "Rationale and challenges for optical interconnects to electronic chips", Proc. IEEE 88, 728 (2000).
- [3]. Rafailov, E. U., Cataluna, M. A. and Sibbett, W., "Mode-locked quantum-dot lasers," Nat. Photonics 1, 395-401 (2007).
- [4]. Liu, G. T., Stintz, A., Li, H., Malloy, K. J. and Lester, L. F., "Extremely low room-temperature threshold current density diode lasers using InAs dots in In_{0.15}Ga_{0.85}As quantum well", Electron. Lett., 35, 1163-1165 (1999).
- [5]. Lin, C. -Y., Xin, Y. -C., Li, Y., Chiragh, F. L. and Lester, L. F., "Cavity design and characteristics of monolithic long-wavelength InAs/InP quantum dash passively mode-locked lasers", Opt. Express, 17, 19739 (2009).
- [6]. Crowley, M. T., Murrell, D., Patel, N., Breivik, M., Lin, C. -Y., Li, Y., Fimland, B. O. and Lester, L. F., "Analytical modeling of the temperature performance of monolithic passively mode – locked quantum dot lasers", IEEE J. Quantum Electron. 47(8), 1059-1068 (2011).
- [7]. Vladimirov, A. G., Turaev, D. and Kozyreff, G., "Delay differential equations for mode – locked semiconductor lasers", Opt. Lett. 29, 1221-1223 (2004).
- [8]. Vladimirov, A. G. and Turaev, D., "New model for mode-locking in semiconductor lasers", Radiophys. Quantum Electron. 47, 769-776 (2004).

- [9]. Vladimirov, A. G. and Turaev, D., "Model for passive mode – locking in semiconductor lasers", *Phys. Rev. A* 72, 033808-1 – 033808-13 (2005).
- [10]. Usechak, N. G., Xin, Y. -C., Lin, C. -Y., Lester, L. F., Kane, D. J. and Kovanis, V., "Modeling and direct electric field measurements of passively mode-locked quantum-dot lasers," *IEEE J. Sel. Top. Quantum Electron.* 15, 653–660 (2009).
- [11]. Erneux, T., [Applied Delay Differential Equations], Surveys and Tutorials in the Applied Mathematical Sciences Vol. 3, Springer, New York (2009).
- [12]. Bandelow, U., Radziunas, M., Sieber, J. and Wolfrum, M., "Impact of gain dispersion on the spatio-temporal dynamics of multisection lasers", *IEEE J. Quantum Electron.*, vol. 37 (2), 183-188 (2001).
- [13]. Rossetti, M., Bardella, P., and Montrosset, I., "Time-domain travelling-wave model for quantum dot passively mode-locked lasers", *IEEE J. Quantum Electron.*, vol. 47(2), 139-150 (2011).
- [14]. Rafailov, E. U., Cataluna, M. A. and Avrutin, E. A., [Ultrafast Lasers Based on Quantum Dot Structures], Wiley-VCH Verlag & Co. KGaA, Weinheim, 132 (2011).
- [15]. Vasil'ev, P., [Ultrafast Diode Lasers: Fundamentals and Applications], Artech House Inc., Boston, 195-199 (1995).
- [16]. Avrutin, E. A. and Russell, B. M., "Dynamics and spectra of monolithic mode-locked laser diodes under external optical feedback," *IEEE J. Quantum Electron.*, vol. 45 (11), 1456-1464 (2009).
- [17]. Melnik, S., Huyet, G. and Uskov, A., "The linewidth enhancement factor α of quantum dot semiconductor lasers", *Opt. Express*, vol. 14(7), 2950-2955 (2006).
- [18]. Newell, T. C., Bossert, D., Stintz, A., Fuchs, B., Malloy, K. J. and Lester, L. F., "Gain and linewidth enhancement factor in InAs quantum dot laser diodes", *IEEE Photon. Technol. Lett.*, vol. 11(12), 1527-1529 (1999).
- [19]. Dagens, B., Markus, A., Chen, J., Provost, J., Make, D., Gouezigou, O. L., Landreau, J., Fiore, A. and Thedrez, B., "Giant linewidth enhancement factor and purely frequency modulated emission from quantum dot laser", *IEEE Electron. Lett.*, vol. 41(6), 323-324 (2005).
- [20]. Blood, P., Lewis, G. M., Smowton, P. M., Summers, H., Thomson, J. and Lutti, J. "Characterization of semiconductor laser gain media by the segmented contact method", *IEEE J. Sel. Top. Quantum Electron.* 9(5), 1275-1282 (2003).
- [21]. Xin, Y. -C., Li, Y., Martinez, A., Rotter, T. J., Su, H., Zhang, L., Gray, A. L., Luong, S., Sun, K., Zou, Z., Zilko, J., Varangis, P. M. and Lester, L. F., "Optical gain and absorption of quantum dots measured using an alternative segmented contact method", *IEEE J. Quantum Electron.* 42, 725-732 (2006).
- [22]. Malins, D. B., Gomez-Iglesias, A., White, S. J., Sibbett, W., Miller, A. and Rafailov, E. U., "Ultrafast electroabsorption dynamics in an InAs quantum dot saturable absorber at 1.3 μm ", *Appl. Phys. Lett.* 89, 171111 (2006).